F. Carbonara, L. Fiore, G. Gialanella, E. Lodi-Rizzini, G. C. Mantovani, M. Napolitano, A. Piazza, A. Piazzoli, R. Rinzivillo, V. Rossi and G. Susinno:
TOTAL AND DIFFERENTIAL CROSS-SECTIONS OF NEGATIVE PION PHOTOPRODUCTION OFF NEUTRONS UP TO 1 GeV. POSSIBLE EVIDENCE FOR THE P_{11} RESONANCE. -

F. Carbonara[(x)], L. Fiore[(o+)], G. Gialanella[(o+)], E. Lodi-Rizzini[(*)],
G. C. Mantovani[(*)], M. Napolitano[(x)], A. Piazza, A. Piazzoli[(*)], R.
Rinzivillo[(x)], V. Rossi[(o)] and G. Susinno : TOTAL AND DIFFEREN-
TIAL CROSS-SECTIONS OF NEGATIVE PION PHOTOPRODUCTION
OFF NEUTRONS UP TO 1 GeV. POSSIBLE EVIDENCE FOR THE
P_{11} RESONANCE. -

We report in this paper some preliminary results on the to-
tal and differential cross-sections of the reaction $\gamma + n \rightarrow p + \pi^-$ ob-
tained by exposing a Deuterium Bubble Chamber to the 1 GeV brems-
strahlung beam of the Frascati electron-synchrotron. In a previous
paper[(1)] we have reported some results concerning the double pion
photoproduction off neutrons, using data obtained in the same experi_
ment.

The main result of this investigation is a significant differen_
ce between the cross-sections of π^+ and π^- photoproduction which ap-
pears in the second-resonance region, if the comparison is made for
the same π-N c. m. energy. Indeed, while the π^+ cross-section shows
the well-known D_{13} peak at 1480 MeV, for the π^- the bump is displa-
ced backwards at about 1400 MeV.

The method of data analysis is very similar to the one descri_
bed in reference (1). The actual measured reaction is $\gamma + d \rightarrow p_s + p + \pi^-$

(x) - Istituto di Fisica dell'Università, Napoli and Istituto Nazionale di
        Fisica Nucleare, Sezione di Napoli
(o) - Istituto di Fisica dell'Università, Roma and Istituto Nazionale di
        Fisica Nucleare, Sezione di Roma.
(+) - Present adress : Istituto Nazionale di Fisica Nucleare, Sezione
        di Napoli
(*) - Istituto di Fisica dell'Università, Pavia and Istituto Nazionale di
        Fisica Nucleare, Gruppo di Pavia.

where p_S is the spectator proton, which is assumed to be the one with the lower momentum.

The events were fitted kinematically with three constraints. When the spectator proton was not visible ($p_S \lesssim 80$ MeV/c) in the cham ber, the standard assumption was made: $p_x = p_y = p_z = 0$ MeV/c and $\Delta p_x = \Delta p_y = 30$ MeV/c, $\Delta p_z = 41$ MeV/c.

7469 events were found which satisfied all the imposed selection criteria ($\chi^2 \leq 10$, $p_S \lesssim 250$ MeV/c, fiducial volume, at least one visible proton besides the π^-, etc.).

The total and differential cross-sections are reported in Table I for 20 intervals of E^{*2}, the c.m. energy squared of the π^--p system.

In the computation of the total and differential cross-sections the loss of events with two invisible protons, as well as the effects due to the possible wrong choise of the spectator proton, were corrected by means of a Monte Carlo calculation. The data at small angles, where the corrections are larger than 25% and the statistics is poor, are quoted without error evaluation and should be considered only as indicative.

No corrections have been made to take into account the effects due to the deuterium target, as the theoretical and experimental information of this subject is still rather poor.

In Fig. 1 the total cross-section as a function of E^{*2} is shown. The superimposed curves represent the total cross-sections for the reactions $\gamma + p \rightarrow \pi^+ + n$ and $\gamma + p \rightarrow \pi^0 + p$. The comparison is made for the same total center-of-mass energy, while the energy scale is al so given, for convenience, in terms of E_γ, the corresponding incident photon energy on free nucleon. The quoted errors are purely statistical; a possible systematic error of the order of 5% on the measured photon flux is not included.

Fig. 2 shows the differential cross-sections for various inter vals of E^{*2} as a function of θ^*, the angle between the π^- and the incident γ-ray in the π^--p c.m. system.

These data are in substantial agreement with those of the ABBHHM collaboration obtained at DESY with the same technique[2].

In Fig. 3 the cross-section at $\theta^* = 90^0$ as a function of E^{*2} is reported. Its behaviour is very similar to that of the total cross-section. The values were obtained by fitting the experimental angular distributions with $\cos \theta^*$ polynomials. The available data from other ex periments are also reported in the figure.

At this point the controversial question of the existence of the P_{11} resonance in π^- photoproduction off neutrons has again to be consi

dered. The experimental angular distributions seem to be in disagree ement with those calculated by Donnachie[4] assuming the presence of the P_{11}. Therefore, we tried to interprete the bump at about 1400 MeV in the total cross-section as due to the D_{13} resonance and to explain the energy shift by means of the interference between this resonance and the Born terms. The calculated effect however is not sufficient to explain the displacement found, so that the cross section bump could be indicative of a relevant P_{11} contribution.

REFERENCES. -

(1) - A. Piazza, G. Susinno, L. Fiore, G. Gialanella, E. Lodi-Rizzini, G. C. Mantovani, A. Piazzoli, F. Carbonara, G. Palomba-Nicco-demi and R. Rinzivillo, Lett. Nuovo Cimento 12, 403 (1970).
(2) - Aachen-Berlin-Bonn-Hamburg-Heidelberg-München collabora-tion, Nuclear Phys. B8, 535 (1968).
(3) - M. Beneventano, F. De Notaristefani, P. Monacelli, L. Paoluzi, F. Sebastiani and M. Severi, Lett. Nuovo Cimento 1, 113 (1969).
(4) - A. Donnachie, Phys. Letters 24B, 420 (1967).

4.

TABLE I

dσ/dΩ*(μb/sr)

	Ex²(GeV²)	Eγ(GeV)	θ*(degrees) σ(μb)	10-20	20-30	30-40	40-50	50-60	60-70	70-80	80-90	90-100	100-110	110-120	120-130	130-140	140-150	150-160	160-170	170-180
I	1.22-1.26	.179-.201	131.2 ±5.2	3.3	3.8	3.9	5.2 ±1.2	6.9 ±1.3	10.6 ±1.5	9.8 ±1.4	10.4 ±1.4	11.9 ±1.5	10.4 ±1.4	10.0 ±1.4	13.6 ±1.8	13.6 ±1.9	11.5 ±1.9	11.6 ±2.3	13.1 ±3.1	15.2 ±5.7
II	1.26-1.30	.201-.222	133.9 ±5.6	2.6	1.0	1.5 ±0.9	5.1 ±1.3	8.9 ±1.6	8.8 ±1.5	10.1 ±1.5	14.6 ±1.8	11.8 ±1.6	11.7 ±1.7	16.3 ±2.0	15.2 ±2.1	12.5 ±2.1	17.4 ±2.6	18.2 ±3.1	11.4 ±3.2	13.0 ±5.8
III	1.30-1.34	.222-.243	162.5 ±6.7	6.7	4.7	3.7 ±1.4	5.3 ±1.4	8.5 ±1.6	9.1 ±1.6	13.6 ±1.8	13.1 ±1.7	13.7 ±1.8	12.0 ±1.8	18.7 ±2.3	21.6 ±2.6	17.8 ±2.5	19.3 ±2.9	17.6 ±3.3	17.6 ±4.2	11.8 ±5.9
IV	1.34-1.38	.243-.265	187.3 ±7.5	4.0	3.4	3.9 ±1.5	8.9 ±1.9	7.7 ±1.6	15.2 ±2.2	13.1 ±2.0	19.6 ±2.4	18.1 ±2.3	18.6 ±2.4	20.3 ±2.5	16.5 ±2.4	19.9 ±2.8	12.5 ±2.5	18.3 ±3.5	22.2 ±5.0	0
V	1.38-1.42	.265-.286	193.4 ±8.1	9.4	2.2	3.6 ±1.5	5.0 ±1.5	6.5 ±1.6	10.7 ±1.9	16.5 ±2.3	13.8 ±2.1	21.6 ±2.6	20.4 ±2.6	16.5 ±2.4	19.4 ±2.7	23.4 ±3.2	21.8 ±3.4	18.5 ±3.7	13.3 ±4.0	3.6 ±3.6
VI	1.42-1.46	.286-.307	215.2 ±9.1	5.2	2.6	4.8 ±1.8	9.7 ±2.3	10.4 ±2.2	18.4 ±2.7	14.6 ±2.4	24.6 ±3.0	25.7 ±3.1	21.1 ±2.9	19.7 ±2.8	15.0 ±2.6	21.5 ±3.4	25.3 ±4.0	20.2 ±4.2	15.8 ±4.8	8.5 ±6.0
VII	1.46-1.50	.307-.328	214.0 ±9.5	0	3.6	5.3 ±2.3	12.4 ±2.7	10.2 ±2.3	23.0 ±3.0	19.9 ±2.9	20.9 ±3.0	20.0 ±2.9	18.1 ±2.8	20.3 ±3.1	21.9 ±3.3	27.2 ±4.0	15.3 ±3.3	10.9 ±3.3	22.6 ±6.0	9.6 ±6.8
VIII	1.50-1.54	.328-.350	177.6 ±9.0	0	1.3	7.7 ±2.6	10.6 ±2.6	15.1 ±2.9	17.7 ±3.0	14.2 ±2.6	17.9 ±2.9	15.6 ±2.7	12.3 ±2.4	17.7 ±3.0	14.5 ±2.8	20.0 ±3.6	19.1 ±3.9	17.3 ±4.3	8.8 ±4.0	5.2 ±5.2
IX	1.54-1.62	.350-.392	167.3 ±6.7	5.7	7.6 ±2.3	9.7 ±2.1	9.9 ±1.9	11.5 ±1.9	10.9 ±1.7	17.1 ±2.1	13.5 ±1.8	15.0 ±1.9	15.2 ±2.0	14.3 ±2.0	15.8 ±2.2	14.4 ±2.3	15.0 ±2.6	12.0 ±2.7	11.8 ±3.4	5.8 ±4.1
X	1.62-1.70	.392-.435	134.7 ±6.5	10.9	9.1 ±2.6	7.4 ±2.0	12.9 ±2.3	14.5 ±2.3	10.2 ±1.8	12.0 ±1.9	13.1 ±2.0	8.7 ±1.6	12.9 ±2.0	10.9 ±1.9	8.1 ±1.7	7.4 ±1.7	9.1 ±2.1	9.6 ±2.6	5.6 ±2.5	6.6 ±4.7
XI	1.70-1.78	.435-.477	102.0 ±6.1	15.0	5.0 ±2.0	7.2 ±2.0	9.6 ±2.1	6.2 ±1.8	9.0 ±1.8	10.2 ±1.8	8.5 ±1.7	9.5 ±1.6	8.4 ±1.7	6.7 ±1.6	8.3 ±1.8	4.3 ±1.4	8.3 ±2.2	8.0 ±2.5	7.9 ±3.2	3.9 ±3.9
XII	1.78-1.86	.477-.520	98.3 ±6.4	0	4.9 ±2.2	12.1 ±2.9	9.6 ±2.3	6.8 ±1.8	12.8 ±2.4	9.5 ±2.0	7.2 ±1.7	8.0 ±1.8	5.8 ±1.5	4.9 ±1.6	5.5 ±1.7	7.9 ±2.1	7.0 ±2.2	4.7 ±2.1	1.5 ±1.5	4.6 ±4.6
XIII	1.86-1.94	.520-.563	87.7 ±6.6	5.4	7.6 ±2.9	9.4 ±2.7	10.7 ±2.6	6.5 ±1.9	8.4 ±2.0	5.6 ±1.6	10.3 ±2.1	5.8 ±1.6	7.9 ±1.9	5.6 ±1.8	9.3 ±2.4	4.4 ±1.7	3.9 ±2.7	2.1 ±1.5	3.5 ±2.4	5.1 ±5.1
XIV	1.94-2.02	.563-.605	99.4 ±7.4	2.9	11.1 ±3.7	9.0 ±2.8	11.6 ±3.2	6.9 ±2.1	8.4 ±2.2	8.5 ±2.1	9.7 ±2.2	8.9 ±2.4	6.3 ±1.8	5.6 ±1.8	8.5 ±2.6	10.7 ±3.1	4.4 ±2.0	4.8 ±2.4	2.0 ±2.0	5.9 ±5.9
XV	2.02-2.10	.605-.648	92.3 ±7.6	7.1	7.5 ±3.4	5.6 ±2.5	7.6 ±2.7	7.7 ±2.4	3.7 ±1.7	1.2 ±2.9	9.5 ±2.5	6.7 ±2.1	7.2 ±2.2	3.5 ±1.9	4.9 ±2.0	10.4 ±3.1	3.3 ±1.9	6.0 ±3.0	4.9 ±3.4	7.2 ±7.2
XVI	2.10-2.18	.648-.690	80.1 ±7.5	3.0	1.6 ±1.6	8.3 ±3.1	5.2 ±2.3	9.8 ±3.0	3.2 ±1.6	7.5 ±2.4	6.7 ±2.1	5.9 ±2.1	4.9 ±1.8	3.2 ±1.6	9.8 ±3.0	4.1 ±2.1	3.8 ±2.2	1.6 ±1.6	0	7.7 ±7.7
XVII	2.18-2.26	.690-.733	67.7 ±7.2	3.1	10.3 ±4.2	5.1 ±2.5	6.2 ±2.5	9.8 ±3.0	3.2 ±1.6	3.7 ±1.6	3.7 ±1.6	4.4 ±1.8	2.3 ±1.3	3.2 ±1.6	1.8 ±1.3	3.1 ±1.8	3.1 ±1.8	6.9 ±3.4	2.8 ±2.8	8.4 ±8.4
XVIII	2.26-2.34	.733-.776	56.3 ±6.7	3.1	5.2 ±3.0	10.3 ±3.6	6.2 ±2.5	2.7 ±1.6	4.9 ±2.0	5.3 ±2.0	2.2 ±1.3	2.0 ±.8	6.1 ±2.2	6.1 ±2.2	3.2 ±1.2	1.8 ±1.3	3.1 ±1.8	8.7 ±3.9	2.8 ±2.8	8.4 ±8.4
XIX	2.34-2.54	.776-.882	43.0 ±3.9	2.7	3.1 ±1.6	3.5 ±1.4	3.8 ±2.2	2.8 ±1.1	5.1 ±1.4	3.8 ±1.1	2.7 ±.9	.9 ±.9	1.7 ±.8	1.5 ±.7	2.2 ±1.5	3.3 ±1.2	5.0 ±2.5	5.5 ±2.1	6.4 ±2.9	7.6 ±5.4
XX	2.54-2.74	.882-.988	33.7 ±5.8	7.2	4.2 ±3.0	3.1 ±2.2		3.2 ±1.9	2.9 ±1.7	3.7 ±1.8	.9 ±.9	.9 ±.9	.9 ±.9	2.9 ±1.7		5.0 ±2.5	3.1 ±2.2	4.2 ±3.0	3.4 ±3.4	0

FIG. 3 – Differential cross-section at $\theta^* =$ = 90° as a function of E^{*2}.
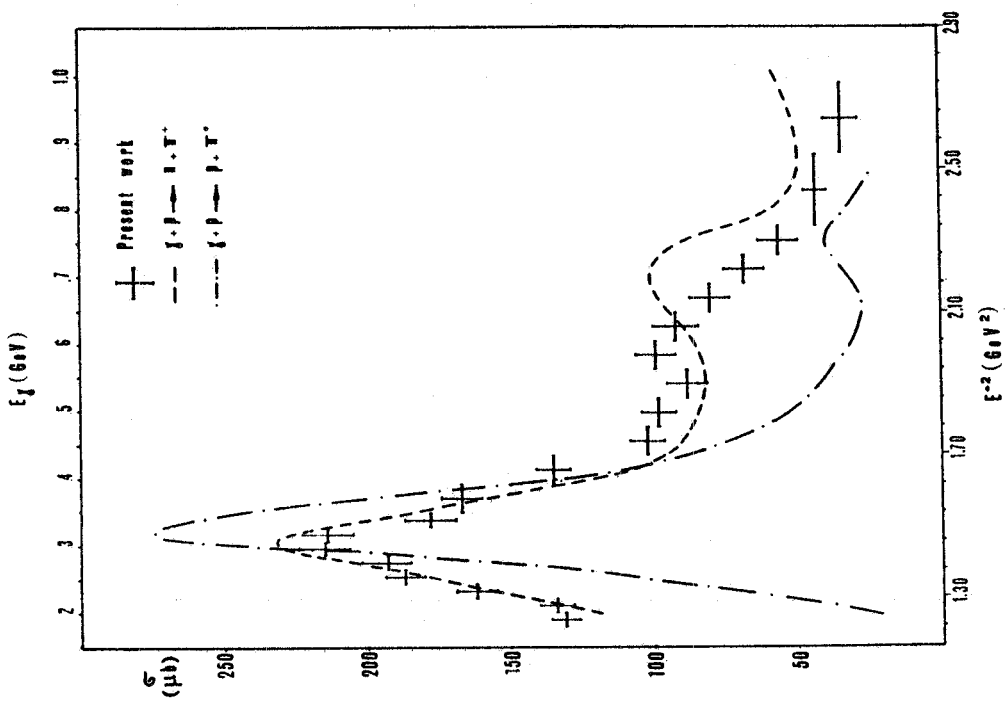

FIG. 1 – Total cross-section for the reaction $\gamma + n \rightarrow p + \pi^-$ as a function of E^{*2} (c. m. energy squared for $\pi^- - p$ system).
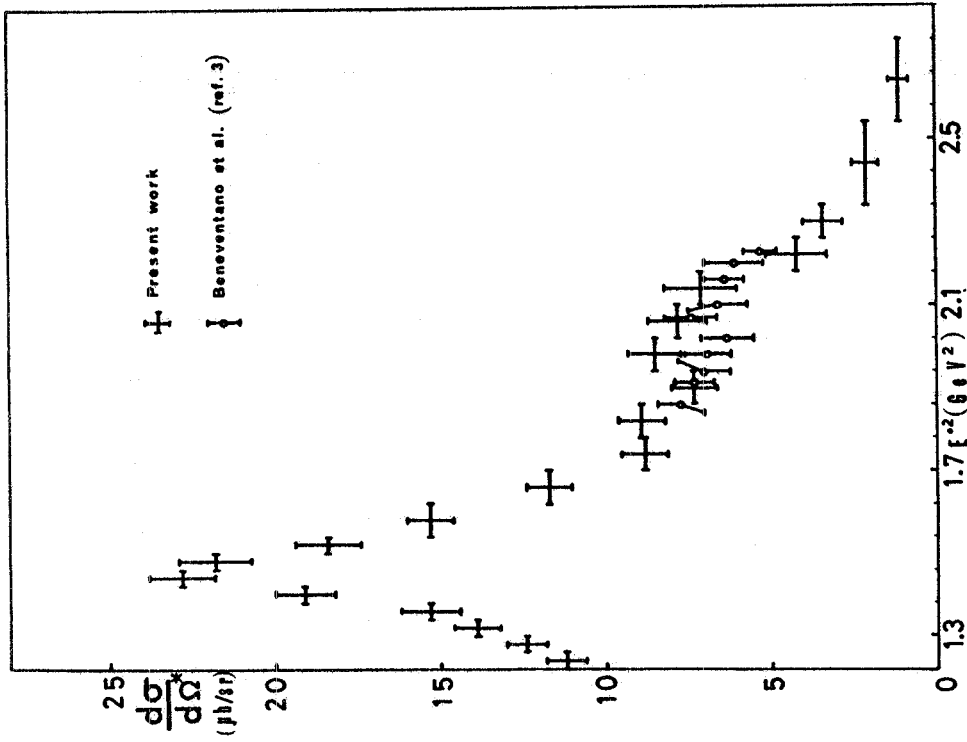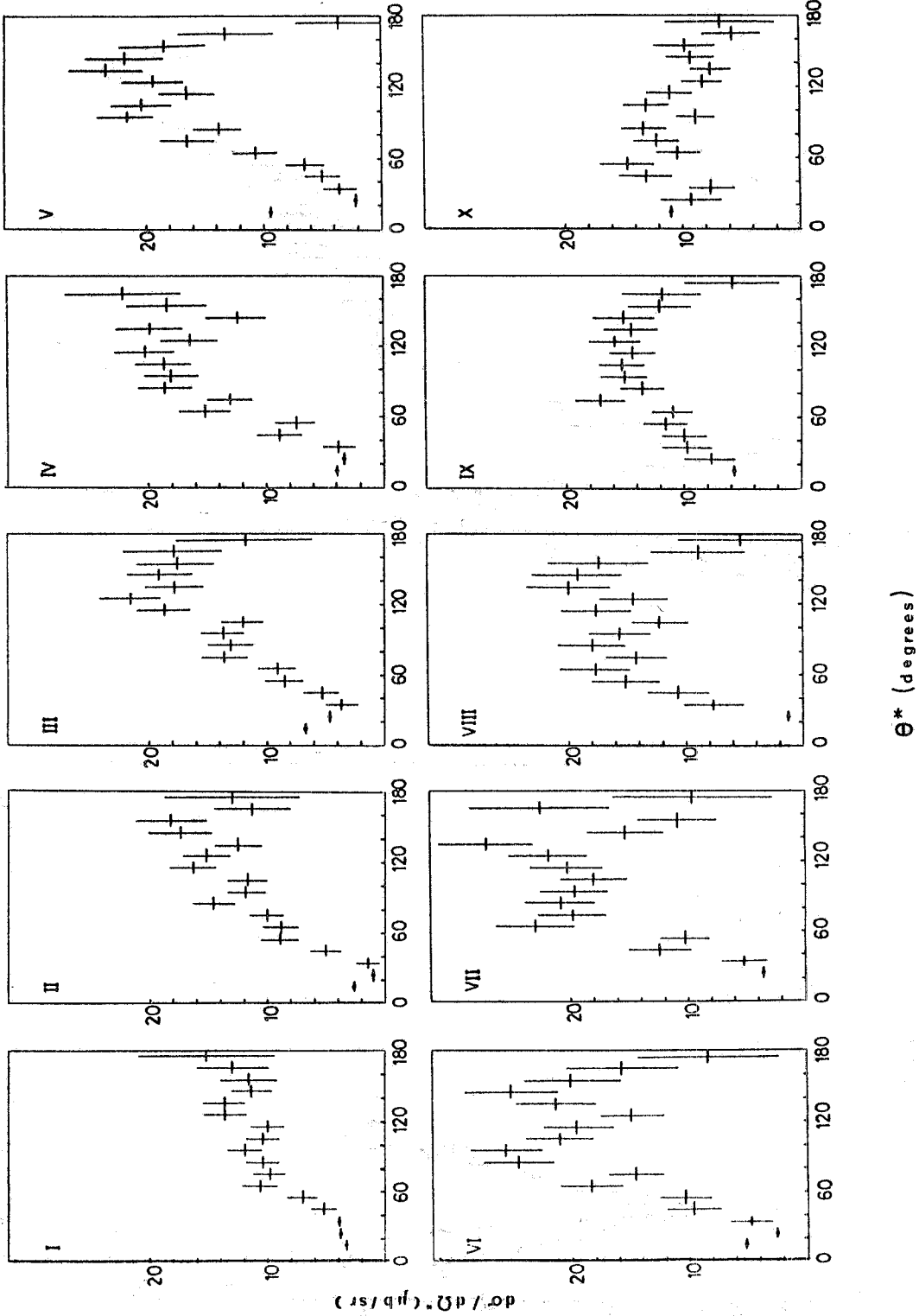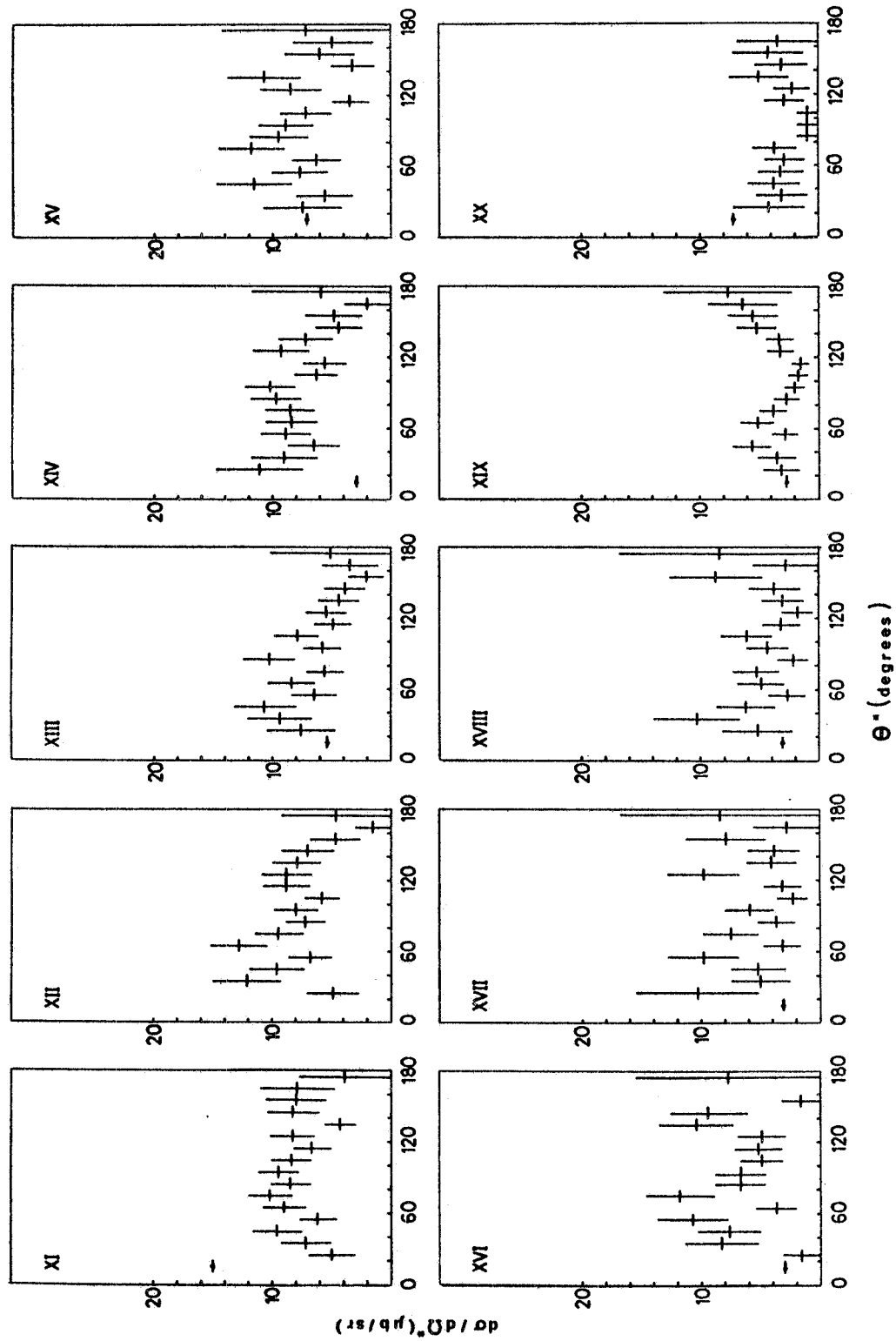
6.

FIG. 2 - Differential cross-section for the I to XX intervals of E^{*2} as a function of θ^*, the angle between the π^- and the incident photon in the π^- - p c. m. s.